Cancer Cell
Article

Argyrin A Reveals a Critical Role for the Tumor Suppressor Protein $p27^{kip1}$ in Mediating Antitumor Activities in Response to Proteasome Inhibition

Irina Nickeleit,[1,10] Steffen Zender,[1,10] Florenz Sasse,[4] Robert Geffers,[5] Gudrun Brandes,[2] Inga Sörensen,[1] Heinrich Steinmetz,[6] Stefan Kubicka,[3] Teresa Carlomagno,[8] Dirk Menche,[7] Ines Gütgemann,[9] Jan Buer,[5] Achim Gossler,[1] Michael P. Manns,[3] Markus Kalesse,[7] Ronald Frank,[4] and Nisar P. Malek[1,3,*]

[1]Institute for Molecular Biology
[2]Institute for Cell Biology
[3]Department of Gastroenterology, Hepatology and Endocrinology
Hannover Medical School, 30625 Hannover, Germany
[4]Department of Chemical Biology
[5]Department of Cell Biology
[6]Research Group Microbial Drugs
[7]Department of Medicinal Chemistry
Helmholtz Centre for Infection Research, 38124 Braunschweig, Germany
[8]Department of NMR-Based Structural Biology, Max Planck Institute for Biophysical Chemistry, 37077 Göttingen, Germany
[9]Department of Pathology, University of Bonn, 53127 Bonn, Germany
[10]These authors contributed equally to this work
*Correspondence: malek.nisar@mh-hannover.de
DOI 10.1016/j.ccr.2008.05.016

SUMMARY

A reduction in the cellular levels of the cyclin kinase inhibitor $p27^{kip1}$ is frequently found in many human cancers and correlates directly with patient prognosis. In this work, we identify argyrin A, a cyclical peptide derived from the myxobacterium *Archangium gephyra*, as a potent antitumoral drug. All antitumoral activities of argyrin A depend on the prevention of $p27^{kip1}$ destruction, as loss of $p27^{kip1}$ expression confers resistance to this compound. We find that argyrin A exerts its effects through a potent inhibition of the proteasome. By comparing the cellular responses exerted by argyrin A with siRNA-mediated knockdown of proteasomal subunits, we find that the biological effects of proteasome inhibition per se depend on the expression of $p27^{kip1}$.

INTRODUCTION

The cyclin kinase inhibitor $p27^{kip1}$ is one of the most frequently dysregulated tumor suppressor proteins in human cancers. Its expression levels closely correlate with the overall prognosis of the affected patient (Porter et al., 2006). In strong contrast to other tumor suppressor proteins, the *$p27^{kip1}$* genomic locus is rarely mutated in cancer cells, indicating that transcriptional and posttranscriptional mechanisms are responsible for the reduction of $p27^{kip1}$ expression (Philipp-Staheli et al., 2001). Since the discovery of skp2 as the essential F box protein that as part of the SCF E3 ubiquitin ligase controls $p27^{kip1}$ stability, several examples of an inverse correlation between skp2 and $p27^{kip1}$ expression in different tumors have been published. Some studies have even shown that tissues from tumors that express low levels of $p27^{kip1}$, i.e., colon carcinoma, mantle cell lymphoma, small-cell lung cancer, and others, also display an increase in $p27^{kip1}$-degradatory activity (Ben-Izhak et al., 2003; Osoegawa et al., 2004). Moreover, a number of molecular treatments like the inhibition of the EGF or ErbB2 receptors, either by inhibitory antibodies or small-molecule drugs, result in increased expression of the $p27^{kip1}$ protein (Lenferink et al., 2000). Together, these findings suggest that an increase in $p27^{kip1}$ expression levels should prevent tumor cell proliferation. To test this possibility,

SIGNIFICANCE

In this work, we identify an antitumoral drug, argyrin A, which acts by stabilizing the cyclin kinase inhibitor $p27^{kip1}$. Due to increased turnover, $p27^{kip1}$ is not sufficiently expressed in many human cancers, and therefore targeting the $p27^{kip1}$ degradation machinery might prove beneficial in the treatment of a variety of human malignancies. We also show that $p27^{kip1}$ belongs to a group of critical substrates that mediate the biological effects of proteasome inhibition. In addition to identifying a $p27^{kip1}$-stabilizing compound, our work improves the understanding of proteasome-regulated processes under normal and pathophysiological conditions.

we recently created a mouse model in which the proteolytic turnover of p27kip1 is partly blocked through a mutation in a p27kip1 phosphorylation site that is critical for ubiquitin-dependent proteasomal turnover (p27T187A) (Malek et al., 2001). When these mice are challenged with a carcinogen (ENU), they develop a variety of tumors with no apparent difference in tumor spectrum compared to wild-type mice. Importantly, however, expression of p27T187A significantly reduces the number of intestinal adenomatous polyps that progress to invasive carcinomas (Timmerbeul et al., 2006). This study therefore showed that preventing p27kip1 degradation could be beneficial in the treatment or prevention of intestinal cancer.

Based on these studies, we set out to identify substances that would reduce or block p27kip1 turnover, thereby allowing re-expression of the protein in tumor tissues.

RESULTS

A Cell-Based Screening Assay Identifies Argyrin A as a Compound that Prevents p27kip1 Degradation

To identify substances that lead to an increase in the expression levels of p27kip1, we generated a high-throughput assay system based on the stable expression of a p27kip1-GFP fusion protein in human cells (see Experimental Procedures for details). One of the substances that exerted the strongest increase in fluorescence was identified as argyrin A, a cyclical peptide that had originally been identified as a metabolic product derived from the myxobacterium *Archangium gephyra* (Sasse et al., 2002) (Figure 1A). The time-course experiment displayed in Figure 1B shows that argyrin A induced an increase in cellular p27kip1 levels in HCT116, SW480, and HeLa cells. To determine whether the argyrin A-induced change in p27kip1 expression levels was due to an increase in its stability, we measured the half-life of p27kip1 in HeLa and SW480 cells in the presence and absence of argyrin A. Figure 1C shows a quantification of the expression levels of p27kip1 compared to actin in cycloheximide-treated cells that were incubated with argyrin A or left untreated. While p27kip1 had a half-life of 4 hr (SW480) or 9 hr (HeLa) in untreated cells, addition of argyrin A blocked the turnover of p27kip1 completely. These results indicate that argyrin A treatment results in an increase in endogenous p27kip1 levels by preventing the turnover of the protein.

As all known p27kip1 turnover mechanisms involve proteolytic destruction of the protein by the 20S proteasome (Montagnoli et al., 1999; Sutterluty et al., 1999), we next measured the activity of purified human proteasomes after incubation with increasing amounts of argyrin A. Figure 2A shows that incubation of purified human 20S proteasome with argyrin A in vitro led to a dose-dependent inhibition of the caspase-, trypsin- and chymotrypsin-like proteasome activities. Importantly, the extent of proteasome inhibition by argyrin A was comparable to that measured with the clinically used proteasome inhibitor bortezomib (Velcade). In agreement with the ability of argyrin A to inhibit the proteasome, we found that other well-known proteasome substrates, namely p53, p21, Bax, and NF-κB, also accumulated in response to argyrin A treatment (Figure 2B). Next we analyzed the cellular effects of argyrin A treatment using a panel of different cell lines. As shown by flow cytometry, argyrin A exerted two different cellular phenotypes (Figure 2C). Primary human fibroblasts and A549

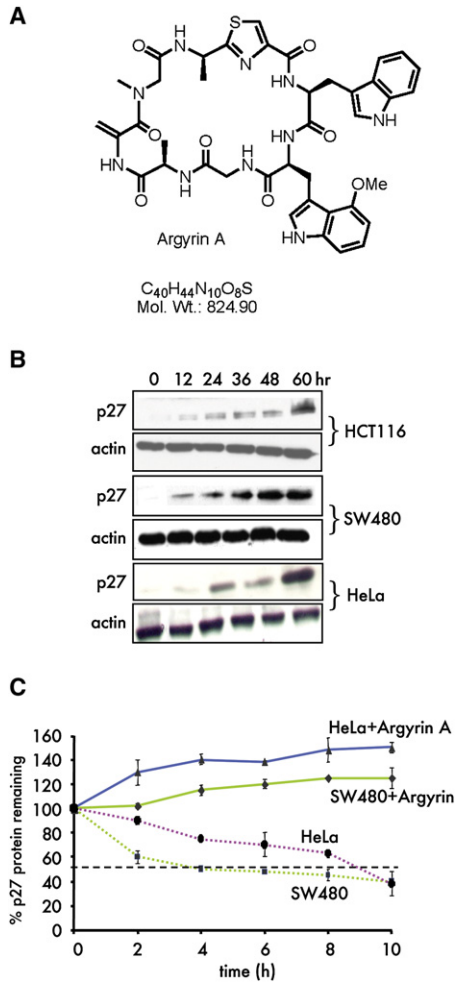

Figure 1. Argyrin A Induces a Decrease in p27kip1 Turnover

(A) Chemical structure of argyrin A.

(B) SW480, HCT116, and HeLa cells were treated with argyrin A to determine the expression levels of p27kip1 by western blotting at the indicated time points.

(C) SW480 and HeLa cells were treated with argyrin A or left untreated for 12 hr, after which cycloheximide was added at a concentration of 25 μg/ml. The expression levels of p27kip1 were determined at the indicated time points by western blotting and normalized against actin expression, which was used as an internal control. The graph shows a quantification of three independent experiments. Error bars represent SD.

and HCT116 cells ceased to proliferate, whereas SW480 and CaCo as well as MCF7 and HeLa cells underwent apoptosis as shown by a dramatic increase in the sub-G1 phase fraction (Figure 2C; see also Figure S1A available online).

Argyrin A-Induced Apoptosis in Tumor Cells Requires the Stabilization of p27kip1

We recently demonstrated that p27kip1 stabilization prevents progression from adenomatous polyps to invasive intestinal cancers (Timmerbeul et al., 2006). We therefore tested whether argyrin A-induced p27kip1 stabilization would be beneficial in the treatment of human colon cancer cell-derived tumor xenografts. We first tested whether argyrin A was active in vivo. After

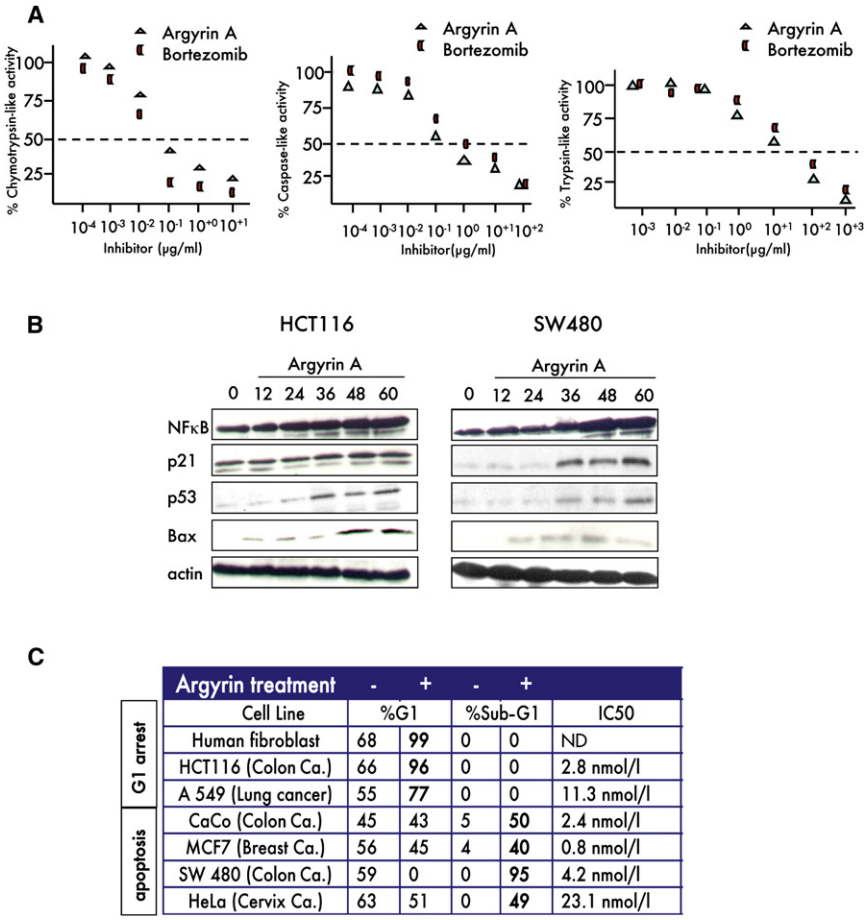

Figure 2. Argyrin A Inhibits the Proteasome

(A) Purified human erythrocyte-derived 20S proteasome was incubated with the indicated amounts of argyrin A or bortezomib, and the caspase-, chymotrypsin-, and trypsin-like proteasome activities were measured using fluorogenic peptide substrates specific for the different catalytic activities.

(B) SW480 and HCT116 cell lines were incubated with argyrin A. At the indicated time points, cells were lysed and the expression levels of p53, p21, Bax, NF-κB, and actin were analyzed by western blotting.

(C) The indicated cell lines were treated with argyrin A, and the G1 and sub-G1 fractions were determined by flow cytometric analysis. IC_{50} values were determined by MTT cell proliferation assays using different concentrations of argyrin A.

intraperitoneal injection of argyrin A, 20S proteasome was isolated from peripheral blood lymphocytes at different time points after injection. As shown in Figure 3A, argyrin A inhibited all proteasome activities. While the maximum inhibitory activity was reached between 24 hr and 48 hr postinjection, all activities returned to baseline levels after 72 hr. Based on this finding, we injected tumor-bearing mice every 3 days with argyrin A (0.15 mg/kg body weight). As shown in Figure 3B, argyrin A led to a significant reduction in the size of the xenotransplanted tumors used in these experiments. The extent and kinetics of tumor regression were comparable to or even more pronounced than that observed in the bortezomib-treated animals. Importantly, however, we did not observe any signs of discomfort, weight loss (Figure 3C), or disease in the argyrin A-treated animals compared to the bortezomib-treated animals. To assay the extent of proteasome inhibition, the induction of $p27^{kip1}$, and the development of apoptotic cell death in primary tumor tissue, we treated tumor-bearing mice with a single dose of argyrin A or bortezomib and explanted tumors at the indicated time points thereafter. As shown in Figure 3D, both bortezomib and argyrin A treatments led to a significant reduction of proteasome activity in the primary tumor tissue. Importantly, argyrin A treatment resulted in induction of $p27^{kip1}$ and apoptotic cell death in more than 60% of all tumor cells (Figures 3E and 3F).

Next we tested whether the stabilization of $p27^{kip1}$ was required for the biological functions associated with argyrin A treatment. To this end, we treated immortalized mouse embryonic fibroblasts (MEFs) from *p27kip1* wild-type or knockout mice with argyrin A or the proteasome inhibitor bortezomib and assayed cell-cycle distribution and apoptosis by flow cytometry. Bortezomib treatment induced apoptosis after 24 hr in both cell lines irrespective of *p27kip1* status, as measured by an increase in the sub-G1 fraction (Figure 4A; Figure S1B). The same response was observed with MG132 treatment (data not shown). In strong contrast, argyrin A treatment induced apoptosis in cells that expressed $p27^{kip1}$ while only 10% of *p27kip1* knockout fibroblasts underwent apoptotic cell death after 60 hr of treatment. These differences in sensitivity in response to argyrin A treatment were not due to differences in the accumulation of other proteasomal substrates in *p27kip1* wild-type and knockout cells, as p53 and p21 levels increased in both cell lines in response to argyrin A (Figure 4B). To extend this observation to human cancer cells, we reduced the levels of $p27^{kip1}$ in HeLa cells using *p27kip1*-specific siRNA. As shown in Figure 4C, HeLa cells expressing $p27^{kip1}$ underwent apoptosis in response to argyrin A after 48 hr of treatment, while cells in which the expression of $p27^{kip1}$ was reduced by pretreatment with *p27kip1* siRNA were protected against the apoptosis-inducing function of this compound.

To gain more insight into the molecular mechanism by which $p27^{kip1}$ induces apoptosis in response to argyrin A treatment, we tested whether this process depends on the cyclin kinase inhibitory function of the $p27^{kip1}$ protein. To answer this question, we used embryonic fibroblasts derived from a *p27kip1* knockin mouse strain that expresses a mutant form of $p27^{kip1}$ that cannot bind cyclin/cdk complexes (p27C-K-) (Besson et al., 2007). Treatment of these cells or wild-type control cells with argyrin A led to the induction of $p27^{kip1}$ expression (Figures S1C and S1D) and apoptosis (Figure 4D). However, suppression of $p27^{kip1}$ expression by siRNA pretreatment protected p27C-K- MEFs against the apoptosis-inducing activity of argyrin A (Figure 4E). These data indicate that the apoptosis-inducing function

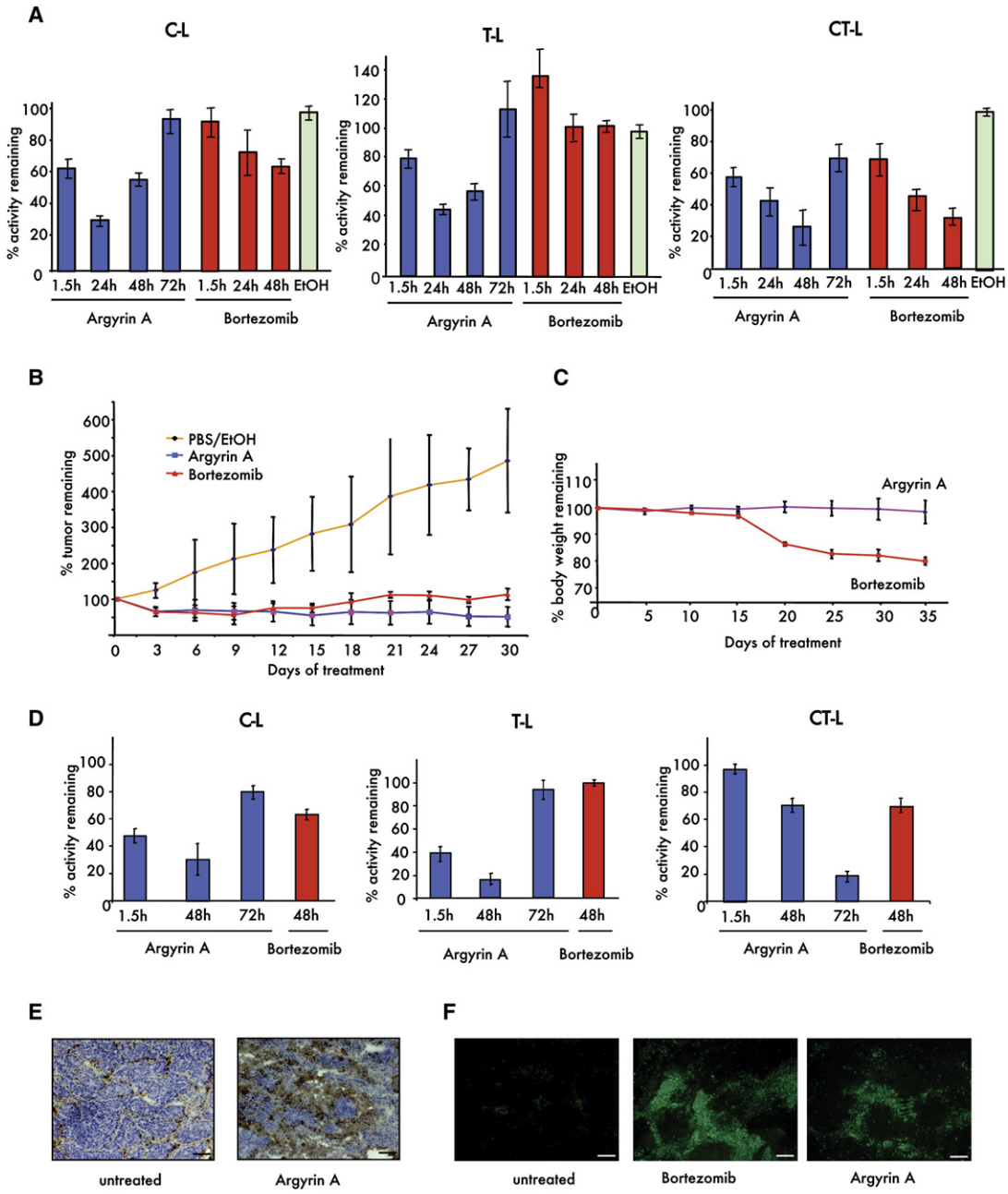

Figure 3. Argyrin A Induces Apoptosis in Human Colon Cancer Xenografts In Vivo

(A) Mice were injected intraperitoneally with argyrin A (0.03 mg/kg body weight) or bortezomib (1 mg/kg body weight). At the indicated time points, 20S proteasome was isolated from peripheral blood cells and the activity of the different proteasome subunits was determined as described in Figure 2A.

(B) SW480 colon carcinoma cell lines mixed with Matrigel were injected under the skin of nu/nu mice to establish xenotransplant tumors. Treatment with argyrin A or bortezomib was begun when these tumors reached a volume of 200 mm^3. The graph shows a quantification of tumor volumes at the indicated time points compared to the starting size, which was set as 100. n = 8 argyrin A (0.15 mg/kg body weight); n = 4 bortezomib (0.6 mg/kg body weight); n = 10 PBS/EtOH control.

(C) All mice were weighed throughout the course of the experiment. The graph shows the changes in body weight for mice treated with argyrin A versus bortezomib.

(D) Determination of proteasome activity in tumor tissue after treatment with bortezomib and argyrin A. After a one-time injection of the respective compounds, tumors were explanted at the indicated time points and proteasomes were extracted from the tumor tissue. The activity of the respective proteasome subunits was determined as described in Figure 2A.

(E) Determination of the number of $p27^{kip1}$-positive cells in tumor tissue after argyrin A treatment. The images show representative samples of immunohistochemical stainings for $p27^{kip1}$ in tumor tissues after 10 days of argyrin A treatment.

(F) Detection of apoptotic cells in xenotransplanted tumors by TUNEL staining of tumor tissues after treatment with argyrin A or bortezomib. At least 200 cells were counted on five independent sections to quantitate the number of apoptotic cells.

Error bars in (A)–(D) represent SD. Scale bars in (E) and (F) = 50 μm.

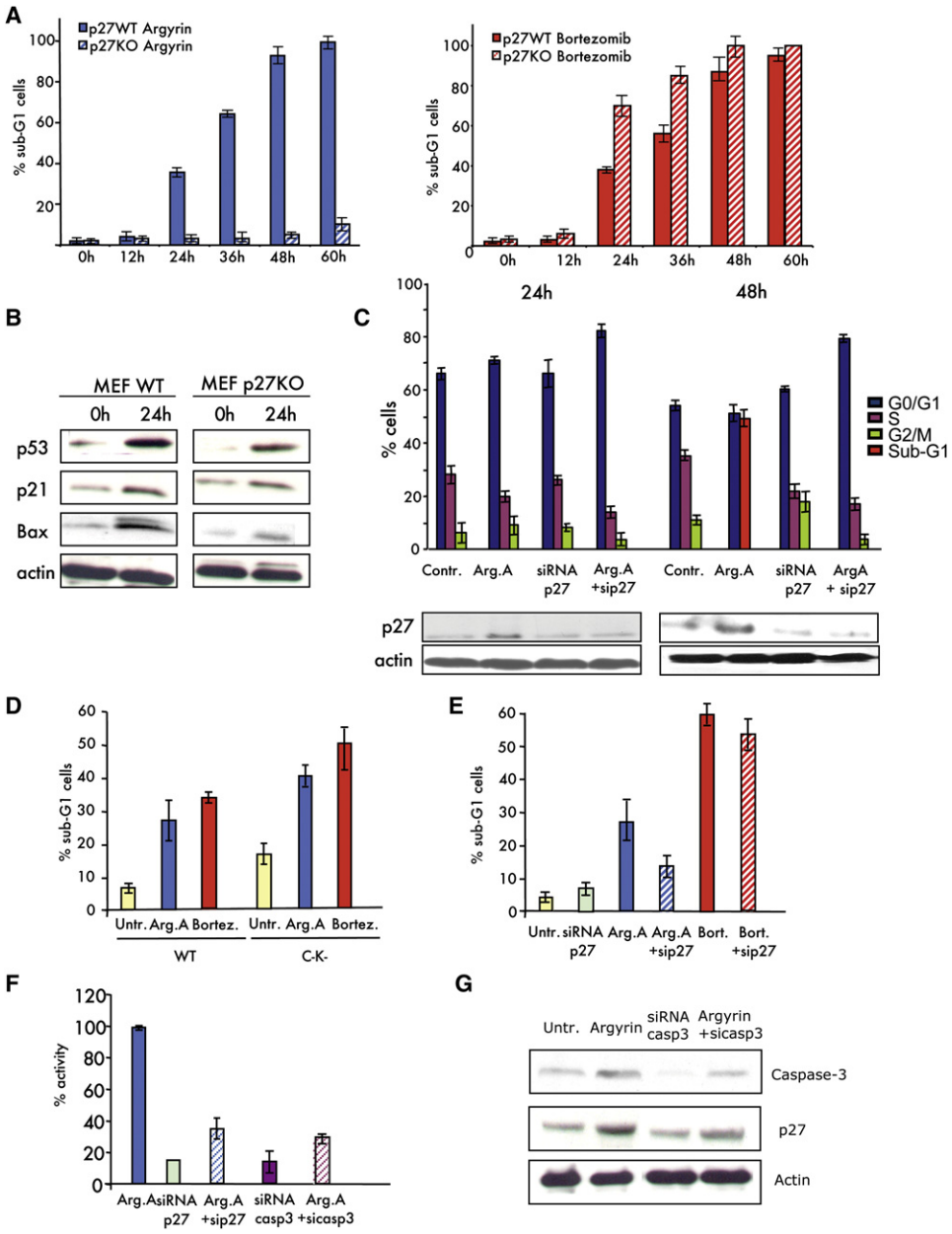

Figure 4. Apoptosis Induced by Proteasome Inhibition Depends on the Expression of p27kip1

(A) Mouse embryonic fibroblasts (MEFs) derived from either wild-type (WT) or *p27kip1* knockout (KO) mice were treated with argyrin A. The number of apoptotic cells was determined by measuring the sub-G1 fraction by flow cytometry. Results shown are the average of six independent experiments.

(B) *p27kip1* wild-type or knockout MEFs were incubated with argyrin A, and the expression levels of p21, p53, Bax, and actin were determined at the indicated time points.

(C) HeLa cells were treated with argyrin A, siRNA against *p27kip1*, or both for either 24 hr (left) or 48 hr (right). The cell-cycle distribution was measured by flow cytometry. The western blots below show the expression levels for p27kip1 in response to the different treatments.

(D) MEFs derived from *p27kip1* wild-type or *p27*C-K- knockin mice (C-K-) were treated with argyrin A or bortezomib or left untreated. The number of apoptotic cells was determined by flow cytometry.

(E) *p27*C-K- MEFs were treated with argyrin A, bortezomib, or siRNA against *p27kip1* as indicated. The number of apoptotic cells was determined by flow cytometry.

(F) Activity of caspase-3 in HeLa cells after treatment with argyrin A, siRNA against caspase-3 (*casp3*), siRNA against *p27kip1*, or the indicated combinations, displayed as % of activity compared to untreated cells.

(G) Western blot analysis of p27kip1, caspase-3, and actin in HeLa cells treated as indicated.

Error bars represent SD.

of p27kip1 in response to proteasome inhibition is independent of its well-characterized function as a cyclin kinase inhibitor.

Proteasome inhibition by argyrin A leads to the stabilization of several different proteins (Figure 2B) that might be involved in the induction of apoptosis in an additive or synergistic manner with p27kip1. Caspase-3, for example, is itself a substrate of the proteasome and a well-known inducer of cell death in response to proteasome inhibition (Suzuki et al., 2001). We therefore asked whether caspase-3 activation is required for the argyrin A-induced and p27kip1-mediated induction of cell death. As shown in Figure 4F, treatment of HeLa cells with argyrin A led to an increase in caspase-3 activity as compared to untreated control cells. Loss of caspase-3 by siRNA treatment protected cells against the apoptosis-inducing activity of argyrin A (Figure 4F) without significantly affecting the levels of p27kip1 (Figure 4G). Loss of p27kip1 in turn prevented the activation of caspase-3 in response to argyrin A treatment (Figure 4F). This experiment establishes caspase-3 as a downstream effector of p27kip1-mediated cell death.

While these results point to a central role of p27kip1 in mediating the apoptosis-inducing function of argyrin A, they do not exclude the possibility that other proteasome-regulated proteins exist that might act in parallel to p27kip1. We therefore tested the importance of IκBα and c-Myc stabilization for the induction of apoptosis in response to argyrin A treatment. The expression of both proteins is controlled by proteasome-mediated degradation, both proteins are regulators of central survival pathways, and both have also been shown to be involved in the control of bortezomib-induced cell death (Adams, 2004a, 2004b; Nikiforov et al., 2007). As shown in Figures S2A and S2B, neither c-Myc nor IκBα knockdown led to a significant reduction in the number of apoptotic MCF7 breast cancer cells after argyrin A treatment.

In summary, these results show that the ability of argyrin A to induce apoptosis in tumor cells depends on the expression of the tumor suppressor protein p27kip1. Interestingly, this profound effect is independent of the cyclin kinase inhibitory function of p27kip1 but involves the activation of caspase-3. While these data point to a central function of p27kip1 in mediating argyrin A-induced cell death, they do not exclude the possibility of parallel independent pathways of equal importance.

Argyrin A-Induced p27kip1 Stabilization Prevents Neovascularization and Damages Existing Tumor Blood Vessels

Next we tested whether argyrin A would also show an effect against HCT116-derived tumor xenografts, as these cell lines did not undergo apoptosis in vitro but instead arrested in the G1 phase. While the reduction in tumor size was not as pronounced as in SW480-derived xenotransplants, we still observed a significant reduction after treatment with argyrin A (Figure 5A). Interestingly, when SW480- or HCT116-derived tumors were explanted, they uniformly showed a large necrotic area in the center of the tumor that was filled with blood and necrotic tumor tissue (Figure 5B). This phenotype is often observed with drugs that interfere with blood vessel formation or compounds that directly damage existing tumor vessels (Tozer et al., 2005).

To analyze this phenotype in greater detail, we first asked whether argyrin A was able to prevent the formation of capillary-like tube structures formed by human umbilical vein endothelial cells (HUVECs) on Matrigel, an assay frequently used to test the ability of a compound to interfere with neovascularization (Maffucci et al., 2005). Figure 5C shows a quantification of the relative length of capillary tubes formed by HUVECs upon stimulation with vascular endothelial growth factor (VEGF). The addition of argyrin A led to a 40% reduction in tube formation in this assay. We then asked whether, in analogy to the results observed for the induction of apoptosis in transformed cells, a reduction of p27kip1 expression levels would protect endothelial cells against the inhibitory activity of argyrin A. Indeed, when HUVECs were transfected with siRNA against *p27kip1* before argyrin A was added, an almost complete rescue of tube length was observed. The effects exerted by bortezomib in this assay were smaller and were not rescued by loss of p27kip1. In addition to tube length, we also quantitated the number of blood vessel-like structures formed by HUVECs after treatment with argyrin A or bortezomib (Figure 5D). Both treatments led to a significant reduction in vessel-like structures. However, loss of p27kip1 only had a significant effect on the argyrin A-induced phenotype, reinforcing the notion that argyrin A exerts its biological functions through an increase in p27kip1 expression. In line with previous observations (Roccaro et al., 2006) showing that proteasome inhibition leads to a reduction in VEGF secretion, we found that both drugs induced an approximately 40% reduction in the expression of VEGF by endothelial cells, which was at least partially rescued by the loss of p27kip1 (Figure 5E). While the reduction in VEGF levels can contribute to the observed antitumoral effects in vivo, the relatively strong increase in VEGF secretion after ablation of p27kip1 by siRNA also suggests that p27kip1 might control the expression levels of VEGF independently of mechanisms affected by proteasome inhibition.

The formation of a necrotic area in the center of a tumor can also be caused by agents that directly target the preexisting tumor vasculature. We therefore determined the microvessel density in tumor tissues (SW480 or HCT116) from mice that received a single injection of argyrin A. Figure 6A shows that argyrin A leads to the induction of p27kip1 expression in CD31-positive endothelial cells as early as 90 min after injection. The increased expression of p27kip1 correlated with a striking reduction of cells that stained positive for CD31, with only about 10% of the positive cells remaining at 72 hr after injection (Figure 6B). Reduction in CD31 staining can be caused by destruction of the endothelial cells or by loss of endothelial function. To understand this phenotype in greater detail, we analyzed primary tumor material by electronic microscopy. As early as 90 min after injection, we observed swelling of endothelial cells that was followed by a loss of basal membrane attachment and cell-cell contacts (Figure 6C) at later time points. As a result, many of the examined tumor blood vessels were occluded with endothelial cells or erythrocytes. The destruction of the tumor core that we observed after argyrin A treatment might therefore be a result of thrombotic occlusion of the affected blood vessels. In contrast, the bortezomib-induced reduction in CD31-positive cells correlated with the appearance of apoptotic endothelial cells (Figure 6C). While many vessel-damaging agents exert their effects through a tubulin-stabilizing activity (Tozer et al., 2005), argyrin A interferes with the ability of the endothelial cell to adhere to the basal membrane. We therefore tested whether argyrin A could also reduce the ability of cultured endothelial cells to form focal adhesions.

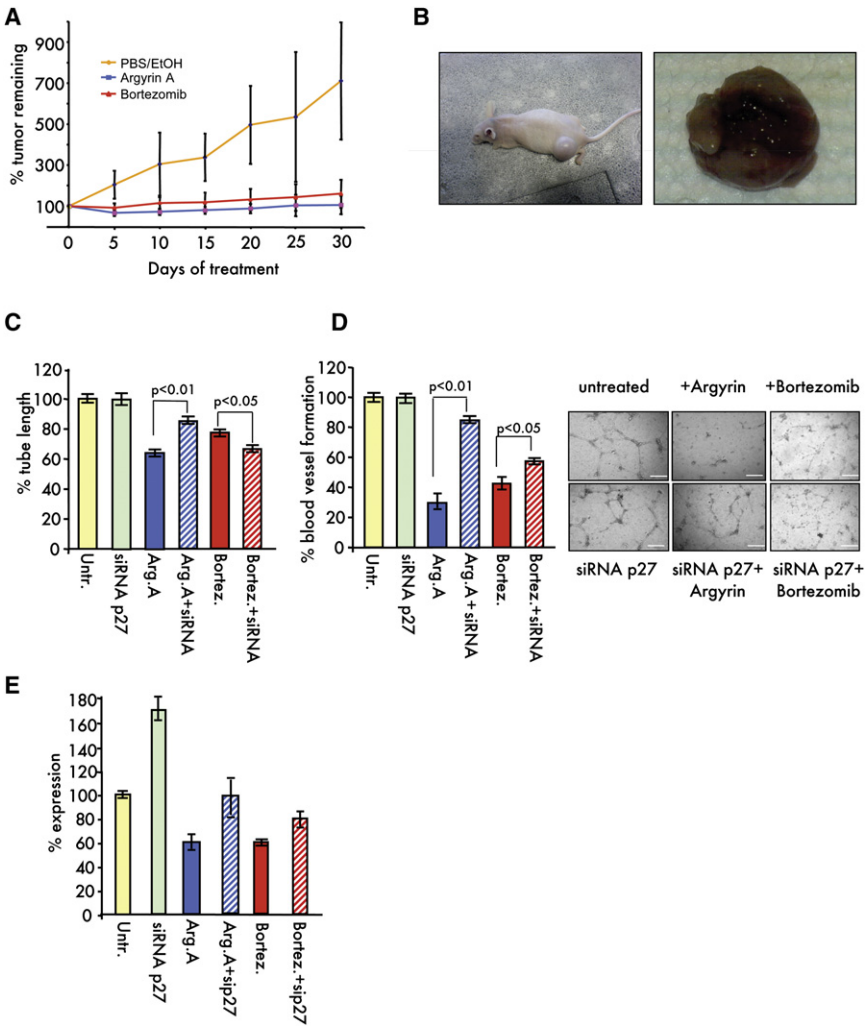

Figure 5. Argyrin A Damages Existing Tumor Blood Vessels and Interferes with Neovascularization in a p27kip1-Dependent Manner

(A) HCT116 colon carcinoma cell lines mixed with Matrigel were injected under the skin of nu/nu mice to establish xenotransplant tumors. Treatment with argyrin A or bortezomib was begun when these tumors reached a volume of 200 mm^3. The graph shows a quantification of tumor volumes at the indicated time points compared to the starting size, which was set as 100. n = 8 argyrin A; n = 8 bortezomib; n = 6 PBS/EtOH.

(B) Macroscopic appearance of a xenotransplant tumor after 10 days of treatment with argyrin A. Note the large necrotic center of the explanted tumor (right).

(C and D) Human umbilical vein endothelial cells (HUVECs) were grown in endothelial cell basal medium supplemented with growth factors and containing 2% FCS for 24 hr and treated with argyrin A (1 μM), bortezomib (10 nM), siRNA against *p27kip1*, argyrin A and siRNA, or bortezomib and siRNA. Tube length (C) and blood vessel-like structures (D) were determined using photographs of HUVEC cultures. The micrographs show representative examples of HUVEC cultures under the indicated conditions. Scale bars = 100 μm.

(E) Expression levels of vascular endothelial growth factor (VEGF) in human endothelial cells after treatment with argyrin A, bortezomib, siRNA against *p27kip1*, or the indicated combinations. Error bars represent SD.

As shown in Figure 6D, staining of human endothelial cells with paxillin antibodies showed a significant reduction in the number of focal adhesions in argyrin A-treated cells as compared to untreated cultures. The reduction in paxillin staining was accompanied by a reduced formation of stress fibers, which were visualized through staining of cultured endothelial cells with antibodies specific for actin. Importantly, both the loss of focal adhesions and the loss of stress fiber formation were reverted when $p27^{kip1}$ expression was reduced with *p27kip1*-specific siRNA before argyrin A was added to the medium.

Stress fiber formation and expression of focal adhesions are both processes regulated through activation of RhoA signaling (Leung et al., 1996; Ridley and Hall, 1992). RhoA activity was therefore directly measured through the use of antibodies that detect the Ser3-phosphorylated form of cofilin, a well-characterized downstream target of RhoA signaling (Besson et al., 2004). Figure 6E shows that treatment with argyrin A reduced the amount of phosphorylated cofilin, while treatment with siRNA against *p27kip1* restores the expression of phosphorylated cofilin completely.

Previous work (Read et al., 1995) had shown that proteasome inhibition due to a reduction in NF-κB activity can also affect integrin signaling, which results in a reduced expression of vascular cell adhesion molecule-1 (VCAM-1) and intercellular adhesion molecule-1 (ICAM-1). As shown in Figures S3A and S3B, treatment of HUVECs with argyrin A or bortezomib led to a reduction in VCAM-1 and ICAM-1 expression, a process that was rescued by the siRNA-mediated suppression of IκBα expression. Interestingly, however, the expression of these proteins was still reduced in argyrin A-treated cells in which $p27^{kip1}$ expression was reduced by siRNA (Figures S3C and S3D). These results indicate that the loss of $p27^{kip1}$ is sufficient to rescue argyrin A-induced changes in cell adhesion despite the inactivation of other central signaling pathways. We conclude that argyrin A exerts its effects on preexisting blood vessels through the stabilization of $p27^{kip1}$ in endothelial cells, which correlates with an inhibition of RhoA signaling. Loss of RhoA signaling induces reduced formation of stress fibers, a reduction in the phosphorylation of downstream effectors, and reduced formation of focal adhesions. These molecular changes provide an explanation for the occlusion of tumor blood vessels in vivo, which resulted in complete destruction of the core of the tumor.

$p27^{kip1}$ Is a Critical Downstream Target of the Proteasome

At this point of our analysis, we had found that argyrin A exerts different antitumoral activities. It induces apoptosis in

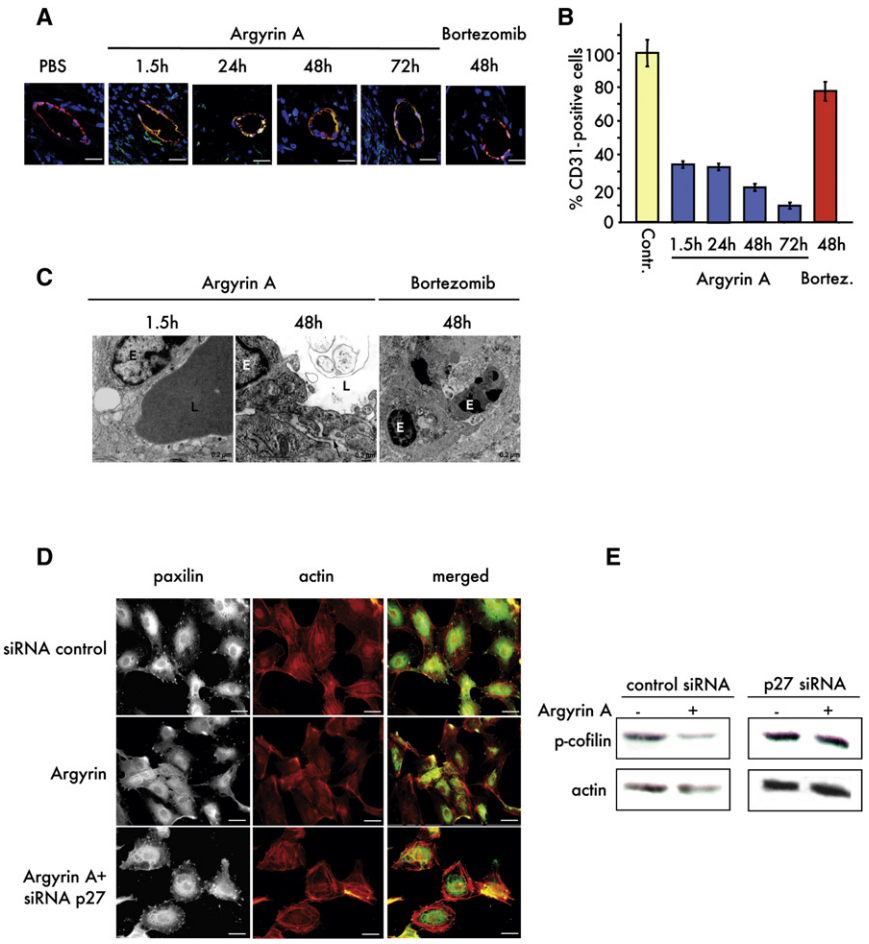

Figure 6. Argyrin A Damages the Existing Tumor Blood Vessels

(A) After a single injection of argyrin A (0.15 mg/kg body weight) or bortezomib (1.0 mg/kg body weight), tumors were explanted at the indicated time points and blood vessels in the tumor tissue were costained for CD31 (red) and p27kip1 (green). Scale bars = 25 μm.

(B) Quantification of the data in (A). Error bars represent SD.

(C) The ultrastructure of microvessels was analyzed after injection of argyrin A (left and middle image) or bortezomib (right image), respectively. Note the swelling of the endothelial cell (E) and the occlusion of the lumen (L) by erythrocytes after 90 min of argyrin A treatment. The black arrow marks the detachment of endothelial cells after 48 hr of argyrin A treatment. The right panel shows apoptotic endothelial cells after treatment with bortezomib.

(D) HUVECs were treated with control siRNA, argyrin A, or argyrin A and siRNA against *p27kip1* as indicated. The cells were fixed and stained with antibodies against paxillin or actin. Scale bars = 25 μm.

(E) HUVECs were treated as indicated, and protein samples were analyzed by western blotting for expression of phosphorylated cofilin. Actin was used as a control.

transformed cells, prevents neovascularization, and leads to a loss of adherence of tumor endothelial cells. All of these activities depend on the expression of p27kip1, while loss of this protein confers resistance to argyrin A treatment. Nevertheless, we found the molecular mechanism by which argyrin A exerts its p27kip1-stabilizing activity to be the inhibition of the 20S proteasome, a multiprotein complex that is involved in the destruction of the majority of all cellular proteins. Moreover, the well-known and clinically used proteasome inhibitor bortezomib showed no specificity for p27kip1 and also differed in its in vitro and in vivo activities from those observed with argyrin A.

We therefore decided to directly test the extent to which the cellular effects of proteasome inhibition per se are influenced by p27kip1 expression. To this end, we designed specific siRNA molecules that target the β1 (caspase-like activity), β2 (trypsin-like activity), and β5 (chymotrypsin-like activity) subunits of the mouse 20S proteasome. We then reduced the expression of these subunits in embryonic fibroblasts derived from wild-type or *p27kip1* knockout cells and measured proteasome activity and cell-cycle distribution. Figures 7A and 7C show activity measurements for the caspase-, chymotrypsin-, and trypsin-like activities of the proteasome after treatment with argyrin A or a combination of siRNAs against the β1, β2, and β5 subunits in *p27kip1* wild-type or knockout cell lines. Importantly, the degree of proteasome inhibition we achieved with siRNA-mediated knockdown of proteasomal subunits was comparable to the effects exerted by argyrin A or bortezomib treatment in vivo (cf. Figure 3A). The levels of proteasome subunit expression are displayed in the corresponding western blots.

Loss of proteasome activity in wild-type fibroblasts led to the induction of apoptosis in approximately 35% (argyrin A) or 45% (siRNA) of all cells after 24 hr (Figure 7B). Importantly, only 5% (argyrin A) or 6% (siRNA) of all fibroblasts derived from *p27kip1* knockout mice underwent apoptosis at comparable levels of proteasome inhibition (Figure 7D), while treatment of wild-type or *p27kip1* knockout cells with bortezomib induced massive apoptosis independent of *p27kip1* status (cf. Figure 4A). These results point toward an as yet unrecognized role of p27kip1 as a critical regulator of apoptotic cell death in response to proteasome inhibition.

To understand in greater detail the mechanisms that make argyrin A-induced cell death dependent upon p27kip1 expression, we decided to compare the cellular responses of cells treated with argyrin A versus bortezomib directly. One way to obtain information on the reaction of a cell toward an external perturbation is to determine the gene expression signature of that cell in response to the perturbation (Lamb et al., 2006). To this end, we determined the gene expression signatures of MCF7 cells in response to argyrin A, bortezomib, or β1,2,5 siRNA and compared the resulting gene expression profiles. Figure 7E shows a Pearson correlation plot of the gene expression data that we obtained in these experiments using untreated or argyrin A-, bortezomib-, or siRNA-treated MCF7 cells. Figure S4A shows

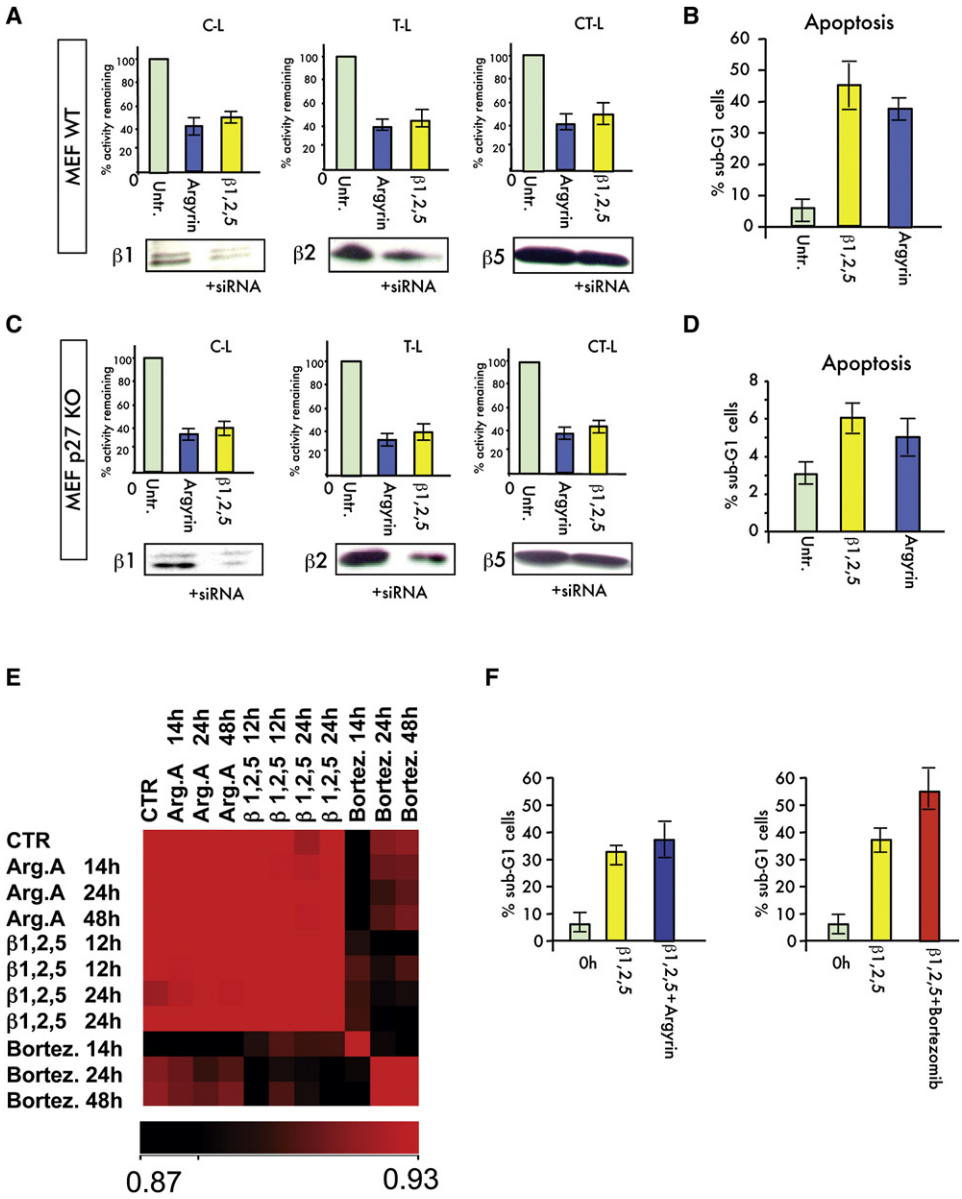

Figure 7. p27kip1 Is Required for the Biological Effect of Proteasome Inhibition

(A and C) Wild-type (A) and *p27kip1* knockout (C) MEFs were treated with argyrin A or transfected with siRNAs specific for the β1, β2, or β5 subunit of the proteasome for 24 hr. Graphs show the remaining catalytic activity of the different proteasome subunits after argyrin A or siRNA treatment compared to an untreated control (n = 3). Western blots below show the expression of the β1, β2, or β5 subunit of the proteasome in proliferating cells before and after treatment with siRNAs for a representative experiment.

(B and D) Flow cytometric measurements of the number of apoptotic cells (sub-G1 fraction) after argyrin A or siRNA treatment in wild-type (B) or *p27kip1* knockout (D) MEFs.

(E) Heat map displaying a correlation analysis of genome-wide gene expression profiles of MCF7 breast cancer cells treated with argyrin A, bortezomib, or siRNA against the β1,2,5 subunits of the proteasome for the indicated amounts of time. The corresponding correlation value matrix is given in Figure S4B.

(F) Number of apoptotic MCF7 cells after transfection with siRNA specific for the β1,2,5 subunits of the proteasome or combined treatment with siRNA and argyrin A or bortezomib. The corresponding proteasome activity measurements are given in Figures S4D and S4E.

the corresponding proteasome activity measurements in MCF7 cells, and Figure S4C shows the correlation values. As shown in Figure 7E, the gene expression profiles of MCF7 cells treated with bortezomib versus argyrin A differ dramatically. While bortezomib treatment led to changes in the expression of more than 10,900 genes (Table S1), only about 500 genes (Table S2) changed in response to argyrin A treatment. Among these genes, 311 were affected by both bortezomib and argyrin A. The functional gene clustering based on their corresponding gene ontology terms (Tables S3A–S3C) indicates that while argyrin A and bortezomib both inhibit the 20S proteasome, they cause very divergent perturbations at the cellular level. From these data,

we conclude that bortezomib treatment affects additional targets in the cell that result in the activation of various cellular responses that make bortezomib-induced cell death independent of $p27^{kip1}$ expression. In a second set of experiments, we compared the gene expression profiles of argyrin A- and siRNA-mediated knockdown of proteasome subunits at comparable levels of proteasome inhibition (Figures S4B and S5; Table S7). These experiments revealed that siRNA-mediated proteasome inhibition, like argyrin A treatment, led to very limited alterations in the gene expression profiles of MCF7 cells (Tables S4 and S5), with approximately 30% of the regulated genes overlapping between argyrin A- and siRNA-treated cells (Figure S6; Table S6). This result indicates that both types of treatment result in few off-target effects. The limited degree of overlap between siRNA- and argyrin A-treated cells may reflect the differences in acute inhibition of proteasome activity by a chemical compound as compared to the reduction in proteasome subunit transcription by siRNA treatment. Our gene expression studies also revealed no evidence for the expression of gene sets associated with the activation of the ER-stress response that has been observed in cells treated with bortezomib (Obeng et al., 2006) (Figure S7).

Finally, we decided to directly test whether the biological activities we observed with argyrin A and bortezomib are at least in part independent of their ability to inhibit the proteasome. To answer this question experimentally, we compared the effects of bortezomib and argyrin A treatment in MCF7 breast cancer cells with cells in which the activity of the proteasome had first been reduced by siRNA-mediated knockdown of the β1, β2, and β5 subunits and which were then treated with argyrin A or bortezomib. Figure 7F shows that argyrin A treatment of cells with reduced proteasome activity did not lead to a significant increase in proteasome inhibition (cf. Figures S4D and S4E for proteasome activity measurements) or in the number of apoptotic cells. Addition of bortezomib to MCF7 cells with reduced proteasome activity also did not increase the level of proteasome inhibition but did result in a >50% increase in the number of apoptotic cells as compared to "pure" proteasome inhibition. These data support the conclusion that bortezomib has cellular effects other than proteasome inhibition that contribute to its biological function.

DISCUSSION

Using a combination of in vitro and in vivo studies, we define three mechanisms by which argyrin A influences tumor cell proliferation, all of which depend on the stabilization of $p27^{kip1}$. By inducing apoptosis, argyrin A can target the tumor cell itself. Previous work pointed to an apoptosis-inducing function of $p27^{kip1}$ overexpression in tumor cells (Katayose et al., 1997; Katner et al., 2002; Wang et al., 1997; Zhang et al., 2005); however, the molecular mechanism by which $p27^{kip1}$ causes cell death is largely unknown. Gene expression profiles of argyrin A-treated MCF7 cells revealed the induction of genes that are involved in the release of cytochrome *c* from the mitochondria, pointing toward a role of the endogenous apoptosis pathway (Table S3A). Importantly, however, the apoptosis-inducing function of argyrin A was entirely dependent on the expression of $p27^{kip1}$, as neither cells derived from *p27kip1* knockout mice nor cells in which $p27^{kip1}$ expression was abolished through siRNA responded to the compound. Nevertheless, $p27^{kip1}$ does not induce apoptosis directly but requires the activation of downstream effectors such as caspase-3. The molecular mechanism by which $p27^{kip1}$ exerts this function is unknown. Surprisingly, however, it does not involve its cyclin kinase inhibitory activity, as cells expressing a non-cdk-binding version of the protein still undergo cell death when treated with argyrin A. This observation is not without precedence, however, as the cyclin kinase inhibitor $p57^{kip2}$ was recently shown to promote apoptosis by activating the intrinsic pathway in response to chemotherapies independently of its cyclin kinase inhibitory function (Vlachos et al., 2007). Our observations therefore add to a growing body of evidence attributing additional functions to the $p27^{kip1}$ protein that are not regulated by the classical cyclin kinase inhibitory activity (Besson et al., 2007; Nguyen et al., 2006; Vernon and Philpott, 2003).

Not all tumor cells that were treated with argyrin A in vitro underwent apoptosis; some instead ceased to proliferate and underwent cell-cycle arrest. A reduction in the proliferative fraction of a tumor is not necessarily beneficial, as quiescent cells are often resistant to chemotherapy or radiation treatment. We therefore tested the extent to which xenotransplanted tumors derived from cells that underwent G1 arrest in response to argyrin A in vitro would still be sensitive to the compound in vivo. We found that such tumors could also be effectively treated. The most prominent change in the tumor tissue was a complete destruction of the core of the cancer, pointing toward an antiangiogenic or vessel-damaging effect of argyrin A. In agreement with previous studies showing that overexpression of $p27^{kip1}$ in human endothelial cells through adenoviral gene transfer reduces cell proliferation (Goukassian et al., 2001), we found that argyrin A reduced the ability of such cells to form vessel-like structures and also reduced the expression of VEGF. This activity was again dependent on the expression of $p27^{kip1}$, as siRNA-transfected endothelial cells became resistant toward treatment with argyrin A and restored VEGF expression.

The third and most surprising antitumoral function of argyrin A is its ability to target preexisting tumor vessels directly. By studying the ultrastructural properties of argyrin A-treated tumors, we found that a single injection of argyrin A induced a loss of adherence of endothelial cells from the basal membrane, which resulted in a protrusion of these cells into the lumen of the vessels. Loss of endothelial cell adhesion was accompanied by signs of thrombosis of the affected tumor vessels. In agreement with these observations in tumor tissues, we found that argyrin A reduces the number of focal adhesions in endothelial cells in vitro by interfering with the activity of RhoA signaling. The role of RhoA in cellular adhesion has been extensively studied, and it was recently shown that $p27^{kip1}$ can control RhoA signaling directly (Besson et al., 2004). *p27kip1* knockout cells show increased levels of RhoA activity, while re-expression of $p27^{kip1}$ inhibits downstream signaling and influences cellular functions like cell migration or adhesion. In line with these observations, we found that the ability of argyrin A to block RhoA signaling and thereby cell adhesion depends on the expression of $p27^{kip1}$. Loss of $p27^{kip1}$ prevents RhoA inhibition by argyrin A and results in the preservation of focal adhesion and stress fiber formation.

Together, these findings show that argyrin A exerts its antitumoral activities through the stabilization of $p27^{kip1}$. This observation is surprising given that our studies indicate that the mechanism by which argyrin A prevents $p27^{kip1}$ turnover is through the

inhibition of the catalytic activities of the 20S proteasome. The proteasome inhibitory activity of argyrin A was demonstrated on purified proteasomes in vitro, in peripheral blood cells in vivo, and in proteasome derived from tumor tissue itself. It encompasses all catalytic activities and is not specific for $p27^{kip1}$, as a number of other proteasomal substrates like p21, p53, and others are no longer degraded in cells treated with argyrin A.

Surprisingly, by blocking proteasome activity with siRNA directed against catalytic proteasomal subunits, we found that $p27^{kip1}$ is indeed required for the apoptosis-inducing function of proteasome inhibition per se. While the proteasome is involved in the regulation of the majority of cellular proteins, our observations regarding the critical role of $p27^{kip1}$ imply that some proteasomal substrates are of key importance in mediating the biological effects connected with proteasome inhibition; one such key substrate is $p27^{kip1}$. The identification of one key proteasome target leads us to speculate that other proteins of equal importance must exist that in an either additive or synergistic manner cause the different biological effects connected with proteasome inhibition.

Our data show that the specificity of argyrin A for $p27^{kip1}$ is not shared by the proteasome inhibitor bortezomib. By comparing the gene expression patterns of argyrin A- and bortezomib-treated cells, we found that the cellular responses exerted by these treatments are highly divergent. Specifically, we found that bortezomib affects a multitude of additional cellular targets that result in a broader biological response of the treated cell. In fact, bortezomib treatment of cells in which the proteasome was partly inhibited through siRNA-mediated reduction in proteasome subunit expression still responded with an increase in the number of apoptotic cells without a further reduction in proteasome activity. In strong contrast, argyrin A- and siRNA-mediated reduction in proteasome activity resulted in only very limited changes in gene expression profiles. The activity and toxicity profile of clinically used inhibitors like bortezomib might therefore not result entirely from the inhibition of the proteasome but may reflect the disruption of additional cellular systems such as the induction of endoplasmic reticulum stress (Obeng et al., 2006). Given that proteasome inhibitors have been shown to synergize with a number of chemotherapeutic or molecular drugs in vitro, it will be important to test whether the greater specificity of argyrin A will allow higher levels of proteasome inhibition at a tolerable level of toxicity.

In summary, we have identified argyrin A as a proteasome inhibitor that by preventing the destruction of the cyclin kinase inhibitor $p27^{kip1}$ exerts broad antitumoral activities. Second, we found that stabilization of $p27^{kip1}$ in addition to targeting the tumor cell itself also affects the tumor vasculature through $p27^{kip1}$-mediated inhibition of RhoA activity. And lastly, we found that $p27^{kip1}$ belongs to a group of critical proteasomal substrates that are responsible for the biological phenotypes induced under conditions of proteasome inhibition. The unique properties of argyrin A combined with its high activity at well-tolerated levels make this compound a good candidate for further clinical development.

EXPERIMENTAL PROCEDURES

High-Throughput Screen for $p27^{kip1}$-Stabilizing Substances

A cellular high-throughput screen for $p27^{kip1}$-stabilizing compounds was established by stably introducing a DNA plasmid (EGFP-N1, Clontech) that allows the expression of $p27^{kip1}$-GFP fusion protein in HeLa cells. $p27^{kip1}$-GFP-expressing cells were selected with neomycin, and several independent clones were subcultured. HeLa $p27^{kip1}$-GFP cells were seeded in 384-well plates (Corning) and incubated with a set of highly diverse natural products (part of the Helmholtz Center for Infection Research myxobacterial metabolite collection) at a concentration of 70 nM. GFP emission was determined by fluorometric measurements using a Victor 1420 multilabel counter (PerkinElmer) at 3 hr, 24 hr, 48 hr, and 60 hr after the start of treatment. The proteasome inhibitor MG132 was used as a positive control. All compounds used for high-throughput screening were dissolved in DMSO at a concentration of 1 mM in 96-well polypropylene microtiter plates. The Helmholtz Center for Infection Research collection of myxobacterial metabolites (Reichenbach and Höfle, 1999) contained 120 pure compounds (>95% pure).

Antibodies, Western Blotting, Immunofluorescence, and Immunohistochemistry

Immunohistochemical staining of mouse tumor tissue, western blotting, cdk2-associated kinase activity measurements, and immunofluorescence experiments were performed as described previously (Kossatz et al., 2006; Timmerbeul et al., 2006). For antibodies used in this study, refer to the Supplemental Data.

siRNA

siRNA knockdown was performed using FuGENE6 or HiPerFect transfection reagent. Transfections were performed using siRNA in a concentration of 0.2 nM for Psmb1, Psmb2, PSMB1, PSMB2, CDKN1B, CASP3, NFKBIA, MYC, and $p27^{kip1}$ and in a concentration of 0.4 nM for Psmb5 and PSMB5.

Proteasome Purification and Proteasome Assays

Proteasome assays with purified 20S proteasome were performed as described previously (Lightcap et al., 2000) using erythrocyte-derived 20S proteasome (Biomol International, LP PW8720) and the fluorometric substrates Succ-LLVY-AMC, BZ-VGR-AMC, and Z-Lle-AMC (Biomol International, LP PW9905). Proteasome extraction from cells and tumor sections was performed as described previously (Crawford et al., 2006). For proteasome extraction from whole blood, frozen whole blood cell pellets were thawed and lysed in 2–3 pellet volumes of cold lysis buffer (5 mM EDTA [pH 8.0]). Lysates were spun down at 4°C, and the supernatant was transferred to a fresh tube. Five microliters was taken for the determination of protein concentration using a Coomassie protein assay (Pierce). Proteasome assays using proteasome purified from cells or tissues were carried out in a 100 μl reaction volume containing 20 μg proteasome extract, 50 mmol/l EDTA, and 60 μmol/l fluorogenic substrate (chymotrypsin-like [CT-L], trypsin-like [T-L], or caspase-like [C-L]) in ATP/DTT lysis buffer at 37°C. The assay buffer was supplemented with a final concentration of 0.05% SDS for the evaluation of the chymotrypsin-like activity and caspase-like activity. The rate of cleavage of fluorogenic peptide substrates was determined by monitoring the fluorescence of released aminomethylcoumarin using a Victor 1420 multilabel counter (Wallac) at an excitation wavelength of 395 nm and emission wavelength of 460 nm over a period of 60 min.

Xenotransplant Studies

All experiments were performed after review by and in accordance with the animal rights and protection agencies of Lower Saxony, Germany. 1×10^7 SW480 cells or HCT116 cells in 100 μl DMEM medium and 100 μl Matrigel were subcutaneously injected into the flanks of NMRI nu/nu mice. Tumors grew for approximately 18 days until they reached an appropriate size (200 mm^3). Tumor size was measured with a digital caliper and calculated with the help of the following formula: (length × [$width^2$]) × π/6.

Electronic Microscopy

Small specimens of tumor were fixed in 2.5% glutaraldehyde (Polysciences) in 0.1 M sodium cacodylate (pH 7.3) and postfixed with 2% osmium tetroxide (Polysciences) in the same buffer. After dehydration in graded alcohols, specimens were embedded in Epon (Serva). Thin sections stained with uranyl acetate and lead citrate were examined in a Philips EM 301 electron microscope. The electron micrographs were selected, digitalized, and processed using Adobe Photoshop 6.0.

DNA Microarray Hybridization and Analysis

DNA microarray hybridization was performed as described previously (Pfoertner et al., 2006). For details on data analysis, please refer to Supplemental Experimental Procedures.

Statistical Analysis

Statistical analysis was carried out using Microsoft Excel software. Unless stated otherwise, all data are presented as mean ± SD; error bars represent SD in all figures. Intergroup comparisons were performed by two-tailed Student's t test. $p < 0.05$ was considered statistical significant.

ACCESSION NUMBERS

The complete data set is deposited in MIAME-compliant format at the NCBI Gene Expression Omnibus (http://www.ncbi.nlm.nih.gov/projects/geo/) and is available under the accession number GSE8565.

SUPPLEMENTAL DATA

The Supplemental Data include Supplemental Experimental Procedures, seven figures, and seven tables and can be found with this article online at http://www.cancercell.org/cgi/content/full/14/1/23/DC1/.

ACKNOWLEDGMENTS

We thank Bettina Hinkelmann and Tanja Töpfer for excellent technical assistance, Maria Höxter for help with FACS analysis, Britta Wieland for supply of cell lines, ChemBioNet for logistical support, H.A. Sundberg Malek for helpful discussions, and Arnaud Besson for p27C-K- MEFs and helpful discussions. This work was supported by grants from the Deutsche Krebshilfe (Max Eder Program) and the Deutsche Forschungsgemeinschaft to N.P.M. and by Bundesministerium für Bildung und Forschung grant 01GR0474 of the German National Genome Research Net (NGFN2) to R.F.

Received: October 30, 2007
Revised: February 14, 2008
Accepted: May 20, 2008
Published: July 7, 2008

REFERENCES

Adams, J. (2004a). The development of proteasome inhibitors as anticancer drugs. Cancer Cell *5*, 417–421.

Adams, J. (2004b). The proteasome: a suitable antineoplastic target. Nat. Rev. Cancer *4*, 349–360.

Ben-Izhak, O., Lahav-Baratz, S., Meretyk, S., Ben-Eliezer, S., Sabo, E., Dirnfeld, M., Cohen, S., and Ciechanover, A. (2003). Inverse relationship between Skp2 ubiquitin ligase and the cyclin dependent kinase inhibitor p27Kip1 in prostate cancer. J. Urol. *170*, 241–245.

Besson, A., Gurian-West, M., Schmidt, A., Hall, A., and Roberts, J.M. (2004). p27Kip1 modulates cell migration through the regulation of RhoA activation. Genes Dev. *18*, 862–876.

Besson, A., Hwang, H.C., Cicero, S., Donovan, S.L., Gurian-West, M., Johnson, D., Clurman, B.E., Dyer, M.A., and Roberts, J.M. (2007). Discovery of an oncogenic activity in p27Kip1 that causes stem cell expansion and a multiple tumor phenotype. Genes Dev. *21*, 1731–1746.

Crawford, L.J., Walker, B., Ovaa, H., Chauhan, D., Anderson, K.C., Morris, T.C., and Irvine, A.E. (2006). Comparative selectivity and specificity of the proteasome inhibitors BzLLLCOCHO, PS-341, and MG-132. Cancer Res. *66*, 6379–6386.

Goukassian, D., Diez-Juan, A., Asahara, T., Schratzberger, P., Silver, M., Murayama, T., Isner, J.M., and Andres, V. (2001). Overexpression of p27(Kip1) by doxycycline-regulated adenoviral vectors inhibits endothelial cell proliferation and migration and impairs angiogenesis. FASEB J. *15*, 1877–1885.

Katayose, Y., Kim, M., Rakkar, A.N., Li, Z., Cowan, K.H., and Seth, P. (1997). Promoting apoptosis: a novel activity associated with the cyclin-dependent kinase inhibitor p27. Cancer Res. *57*, 5441–5445.

Katner, A.L., Hoang, Q.B., Gootam, P., Jaruga, E., Ma, Q., Gnarra, J., and Rayford, W. (2002). Induction of cell cycle arrest and apoptosis in human prostate carcinoma cells by a recombinant adenovirus expressing p27(Kip1). Prostate *53*, 77–87.

Kossatz, U., Vervoorts, J., Nickeleit, I., Sundberg, H.A., Arthur, J.S., Manns, M.P., and Malek, N.P. (2006). C-terminal phosphorylation controls the stability and function of p27kip1. EMBO J. *25*, 5159–5170.

Lamb, J., Crawford, E.D., Peck, D., Modell, J.W., Blat, I.C., Wrobel, M.J., Lerner, J., Brunet, J.P., Subramanian, A., Ross, K.N., et al. (2006). The Connectivity Map: using gene-expression signatures to connect small molecules, genes, and disease. Science *313*, 1929–1935.

Lenferink, A.E., Simpson, J.F., Shawver, L.K., Coffey, R.J., Forbes, J.T., and Arteaga, C.L. (2000). Blockade of the epidermal growth factor receptor tyrosine kinase suppresses tumorigenesis in MMTV/Neu + MMTV/TGF-alpha bigenic mice. Proc. Natl. Acad. Sci. USA *97*, 9609–9614.

Leung, T., Chen, X.Q., Manser, E., and Lim, L. (1996). The p160 RhoA-binding kinase ROK alpha is a member of a kinase family and is involved in the reorganization of the cytoskeleton. Mol. Cell. Biol. *16*, 5313–5327.

Lightcap, E.S., McCormack, T.A., Pien, C.S., Chau, V., Adams, J., and Elliott, P.J. (2000). Proteasome inhibition measurements: clinical application. Clin. Chem. *46*, 673–683.

Maffucci, T., Piccolo, E., Cumashi, A., Iezzi, M., Riley, A.M., Saiardi, A., Godage, H.Y., Rossi, C., Broggini, M., Iacobelli, S., et al. (2005). Inhibition of the phosphatidylinositol 3-kinase/Akt pathway by inositol pentakisphosphate results in antiangiogenic and antitumor effects. Cancer Res. *65*, 8339–8349.

Malek, N.P., Sundberg, H., McGrew, S., Nakayama, K., Kyriakides, T.R., and Roberts, J.M. (2001). A mouse knock-in model exposes sequential proteolytic pathways that regulate p27Kip1 in G1 and S phase. Nature *413*, 323–327.

Montagnoli, A., Fiore, F., Eytan, E., Carrano, A.C., Draetta, G.F., Hershko, A., and Pagano, M. (1999). Ubiquitination of p27 is regulated by Cdk-dependent phosphorylation and trimeric complex formation. Genes Dev. *13*, 1181–1189.

Nguyen, L., Besson, A., Heng, J.I., Schuurmans, C., Teboul, L., Parras, C., Philpott, A., Roberts, J.M., and Guillemot, F. (2006). p27kip1 independently promotes neuronal differentiation and migration in the cerebral cortex. Genes Dev. *20*, 1511–1524.

Nikiforov, M.A., Riblett, M., Tang, W.H., Gratchouck, V., Zhuang, D., Fernandez, Y., Verhaegen, M., Varambally, S., Chinnaiyan, A.M., Jakubowiak, A.J., and Soengas, M.S. (2007). Tumor cell-selective regulation of NOXA by c-MYC in response to proteasome inhibition. Proc. Natl. Acad. Sci. USA *104*, 19488–19493.

Obeng, E.A., Carlson, L.M., Gutman, D.M., Harrington, W.J., Jr., Lee, K.P., and Boise, L.H. (2006). Proteasome inhibitors induce a terminal unfolded protein response in multiple myeloma cells. Blood *107*, 4907–4916.

Osoegawa, A., Yoshino, I., Tanaka, S., Sugio, K., Kameyama, T., Yamaguchi, M., and Maehara, Y. (2004). Regulation of p27 by S-phase kinase-associated protein 2 is associated with aggressiveness in non-small-cell lung cancer. J. Clin. Oncol. *22*, 4165–4173.

Pfoertner, S., Jeron, A., Probst-Kepper, M., Guzman, C.A., Hansen, W., Westendorf, A.M., Toepfer, T., Schrader, A.J., Franzke, A., Buer, J., and Geffers, R. (2006). Signatures of human regulatory T cells: an encounter with old friends and new players. Genome Biol. *7*, R54.

Philipp-Staheli, J., Payne, S.R., and Kemp, C.J. (2001). p27(Kip1): regulation and function of a haploinsufficient tumor suppressor and its misregulation in cancer. Exp. Cell Res. *264*, 148–168.

Porter, P.L., Barlow, W.E., Yeh, I.T., Lin, M.G., Yuan, X.P., Donato, E., Sledge, G.W., Shapiro, C.L., Ingle, J.N., Haskell, C.M., et al. (2006). p27(Kip1) and cyclin E expression and breast cancer survival after treatment with adjuvant chemotherapy. J. Natl. Cancer Inst. *98*, 1723–1731.

Read, M.A., Neish, A.S., Luscinskas, F.W., Palombella, V.J., Maniatis, T., and Collins, T. (1995). The proteasome pathway is required for cytokine-induced endothelial-leukocyte adhesion molecule expression. Immunity *2*, 493–506.

Reichenbach, H., and Höfle, G. (1999). Myxobacteria as producers of secondary metabolites. In Drug Discovery from Nature, S. Grabley and R. Thieriecke, eds. (Berlin: Springer Verlag), pp. 149–179.

Ridley, A.J., and Hall, A. (1992). The small GTP-binding protein rho regulates the assembly of focal adhesions and actin stress fibers in response to growth factors. Cell *70*, 389–399.

Roccaro, A.M., Hideshima, T., Raje, N., Kumar, S., Ishitsuka, K., Yasui, H., Shiraishi, N., Ribatti, D., Nico, B., Vacca, A., et al. (2006). Bortezomib mediates antiangiogenesis in multiple myeloma via direct and indirect effects on endothelial cells. Cancer Res. *66*, 184–191.

Sasse, F., Steinmetz, H., Schupp, T., Petersen, F., Memmert, K., Hofmann, H., Heusser, C., Brinkmann, V., von Matt, P., Hofle, G., and Reichenbach, H. (2002). Argyrins, immunosuppressive cyclic peptides from myxobacteria. I. Production, isolation, physico-chemical and biological properties. J. Antibiot. (Tokyo) *55*, 543–551.

Sutterluty, H., Chatelain, E., Marti, A., Wirbelauer, C., Senften, M., Muller, U., and Krek, W. (1999). p45SKP2 promotes p27Kip1 degradation and induces S phase in quiescent cells. Nat. Cell Biol. *1*, 207–214.

Suzuki, Y., Nakabayashi, Y., and Takahashi, R. (2001). Ubiquitin-protein ligase activity of X-linked inhibitor of apoptosis protein promotes proteasomal degradation of caspase-3 and enhances its anti-apoptotic effect in Fas-induced cell death. Proc. Natl. Acad. Sci. USA *98*, 8662–8667.

Timmerbeul, I., Garrett-Engele, C.M., Kossatz, U., Chen, X., Firpo, E., Grunwald, V., Kamino, K., Wilkens, L., Lehmann, U., Buer, J., et al. (2006). Testing the importance of p27 degradation by the SCFskp2 pathway in murine models of lung and colon cancer. Proc. Natl. Acad. Sci. USA *103*, 14009–14014.

Tozer, G.M., Kanthou, C., and Baguley, B.C. (2005). Disrupting tumour blood vessels. Nat. Rev. Cancer *5*, 423–435.

Vernon, A.E., and Philpott, A. (2003). A single cdk inhibitor, p27Xic1, functions beyond cell cycle regulation to promote muscle differentiation in Xenopus. Development *130*, 71–83.

Vlachos, P., Nyman, U., Hajji, N., and Joseph, B. (2007). The cell cycle inhibitor p57(Kip2) promotes cell death via the mitochondrial apoptotic pathway. Cell Death Differ. *14*, 1497–1507.

Wang, X., Gorospe, M., Huang, Y., and Holbrook, N.J. (1997). p27Kip1 overexpression causes apoptotic death of mammalian cells. Oncogene *15*, 2991–2997.

Zhang, Q., Tian, L., Mansouri, A., Korapati, A.L., Johnson, T.J., and Claret, F.X. (2005). Inducible expression of a degradation-resistant form of p27Kip1 causes growth arrest and apoptosis in breast cancer cells. FEBS Lett. *579*, 3932–3940.